EVOLUTIONARY ALGORITHMS FOR THE IDENTIFICATION OF STRUCTURAL SYSTEMS IN EARTHQUAKE ENGINEERING

Anastasia Athanasiou[1], Matteo De Felice[2], Giuseppe Oliveto[1] and Pietro S. Oliveto[3]
[1]*Institute of Structural Engineering, University of Catania, Catania, Italy*
[2]*Energy and Environment Modeling Technical Unit, ENEA, Rome, Italy*
[3]*School of Computer Science, University of Birmingham, Birmingham, U.K.*

Keywords: Earthquake engineering, Structural system identification, Evolution strategies, CMA-ES, Real-world applications.

Abstract: An application of Evolution Strategies (ESs) to the structural identification of base isolation systems in earthquake engineering is presented. The analysis of a test problem considered in the literature clearly shows the effectiveness of ESs for the problem. Simple ESs outperform the previously used methods while state-of-the-art ones, such as the CMA-ES, provide practically exact solutions. The application of the CMA-ES to the real data recorded in 2004, when releasing imposed displacements on a building in Solarino, leads to improved identification results and gives hints of limitations in the model available in literature. Improved models of higher dimensionality are introduced to overcome such limitations. The application of the CMA-ES with the new models leads to improvements of up to 53% compared to the previous solutions in literature. Thus, ESs are shown to be a very powerful tool for the dynamic identification of structural systems and an important aid in the design and evaluation of models of high dimensionality for structure identification.

1 INTRODUCTION

Structural engineering is a special technological field dealing with the analysis and design of engineering structures that must resist internal and/or external loads. Such structures may be integral parts of buildings, bridges, dams, ship hulls, aircraft, engines and so on. The design of such structures is an optimisation process by which the resistance capacity of the system is made to meet the demands posed to it by the environment. This process is based on the satisfaction of the basic design inequality by which the capacity must be no lower than the demand. While the capacity can be established by the engineer at each step of the design process, the demand depends both on the characteristics of the system itself and on its interaction with the surrounding environment.

The evaluation of the demands requires the simulation of the behaviour of the structural system (i.e. the *response*) under service and/or extreme loading conditions (eg. earthquakes, tornadoes, turbulence etc). Such simulations require the construction of mechanical models which enable the prediction of the system's behaviour. Usually a mechanical model is described by a system of linear or non-linear differential equations and a set of physical parameters. While the system of differential equations is derived from first principles in mechanics, the physical parameters are derived from laboratory tests on materials and/or on structural parts of the system.

Structural identification can serve the dual purpose of establishing whether a given model is suitable to describe the behaviour of a structural system or to verify that the physical parameters fed into a reliable model correspond to the characteristics of the actual materials used in the construction of the system.

Base isolation is a modern system for the protection of buildings and other constructions against earthquake excitations and works on the principle of decoupling the motion of the ground from that of the building. Ideally the building should stay still while the ground moves beneath it. This is achieved by interposing a set of special bearings (i.e. *seismic isolators*) between the foundation and the superstructure.

Given the low stiffness of the building structure due to the presence of the seismic isolators it is rather easy to displace (i.e. move) the building by pushing it at the base with suitable actuators (i.e. *hydraulic jacks*). This system has been used in a handful of applications around the world (see the literature re-

Athanasiou A., De Felice M., Oliveto G. and S. Oliveto P..
EVOLUTIONARY ALGORITHMS FOR THE IDENTIFICATION OF STRUCTURAL SYSTEMS IN EARTHQUAKE ENGINEERING.
DOI: 10.5220/0003672900520062
In *Proceedings of the International Conference on Evolutionary Computation Theory and Applications* (ECTA-2011), pages 52-62
ISBN: 978-989-8425-83-6

view in (Oliveto et al., 2010) and references (15–19) therein) including one in the town of Solarino in Eastern Sicily (Oliveto et al., 2010).

The Solarino building was tested by release of imposed displacements in July 2004 and accelerations were recorded at each floor. These recordings were used as response functions for the identification of the base isolation system (Oliveto et al., 2010).

An iterative procedure based on the least squares method was used in (Oliveto et al., 2010) for the identification. This required tedious calculations of gradients which were done approximately by means of an ingenious numerical procedure. Before applying the identification procedure to the experimental data, the same procedure was evaluated against a test problem for which the solution was known. Hence, the ability of the optimisation algorithm was assessed in the absence of measurement noise and with the guarantee that the function to be identified fits the model. The procedure, was then applied to the real data derived from the tests on the Solarino building.

Although, the authors of (Oliveto et al., 2010) are satisfied with their results, they conclude that a "need for improvement both in the models and testing procedures also emerges from the numerical applications and results obtained". In particular, finding the "best" algorithm for the identification of such a kind of problem would provide an improvement on the state-of-the-art on the identification of building and structures from dynamic tests.

In this paper the described problem is addressed by applying Evolutionary Algorithms (EAs) for the identification of structural engineering systems. Indeed, the first applications of evolution computations were directed towards parameter optimisation for civil engineering simulation models e.g. simulating stress and displacement patterns of structures under load (Schwefel, 1993).

Firstly, the performance of well known evolutionary algorithms for numerical optimization (i.e. Evolution Strategies (ESs)) is evaluated on the same test problem considered in (Oliveto et al., 2010). Several ESs are applied and their performance is compared amongst themselves and against the previous results obtained in (Oliveto et al., 2010). It is shown that even simple ESs outperform the previously used methods, while state-of-the-art ones such as the CMA-ES, provide solutions improved by several orders of magnitude, practically the exact solution.

By applying efficient ESs to the real data from the Solarino experiments, further and convincing evidence is given of the limitations of the model for the identification of the base isolation system. Such limitations could not be as visible from the results obtained with the previously used optimisation methods. Finally, new improved models designed to overcome the limitations exhibited by the previous ones are tested. It is stressed that application simplicity and performance reliability of ESs allowed to evaluate improved models of higher dimensionality in a much smaller amount of time than otherwise would have been required.

The paper is structured as follows. The system identification problem is described in Section 2 where previous results are presented together with a brief introduction of ESs. A comparative study is performed on the test problem in Section 3. The best performing ESs are applied in Section 4 to data from experimental tests on the Solarino building. Two new models for the identification of hybrid base-isolation systems are presented in Section 5 together with the results obtained from the identification of the Solarino building. In the final section conclusions are drawn.

2 PRELIMINARIES

2.1 The Mechanical Model

The mechanical model simulating the experiments performed on the Solarino building is provided by the one degree of freedom system shown in Fig. 1. The justification for its use can be found in (Oliveto et al., 2010). The mechanical model consists of a mass restrained by a bi-linear spring (BS) in parallel with a linear damper (LD) and a friction device (FD). Fig. 1 (a) describes the mechanical system, while Fig. 1 (b) shows the constitutive behaviour of the bi-linear spring (modelling rubber bearings). Fig. 1 (c) shows the relationship between the force in the friction device and the corresponding displacement (modelling sliding bearings).

The mechanical model is governed by the following second order ordinary differential equation

$$m \cdot \ddot{u} + c \cdot \dot{u} + f_s(u, \dot{u}) + f_d \cdot sign(\dot{u}) = 0 \qquad (1)$$

where c is the constant of the linear damper (LD), f_d is the dynamic friction force in the friction device while $\dot{u}$ and $\ddot{u}$ are respectively the first and the second derivatives of the displacement $u(t)$ with respect to time. Physically, the derivatives represent the velocity ($\dot{u}$) and the acceleration ($\ddot{u}$) of the mass m of the building. Finally, the restoring force in the bi-linear spring $f_s(u, \dot{u})$ depends on the various phases of motion of the mechanical model, that is the various branches shown in Fig. 1 (b):

$$f_s(u, \dot{u}) = k_0 \cdot [u - u_i - u_y \cdot sign(\dot{u})] + k_1 \cdot [u_i + u_y \cdot sign(\dot{u})]$$

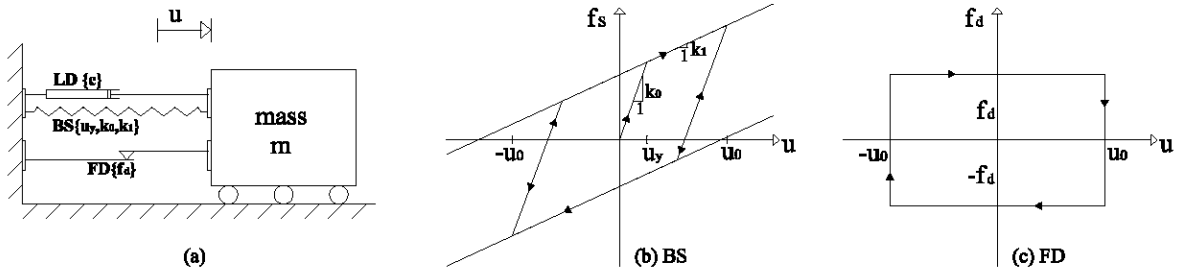

Figure 1: The mechanical model: (a) mechanical system: (b) constitutive behaviour of the bi-linear spring; (c) friction force-displacement relationship.

for the branches of slope k_0 and

$$f_s(u,\dot{u}) = k_0 \cdot u_y \cdot sign(\dot{u}) + k_1 \cdot [u - u_y \cdot sign(\dot{u})]$$

for the branches of slope k_1. In the above equations u_i is the displacement at the beginning of the considered phase of motion while u_y is the yield displacement of the bi-linear spring as shown in Fig. 1 (b). The equation of motion (1), is supplemented by the following two initial conditions which are implicit to the considered experiment:

$$u(t_0) = u_0 \qquad \dot{u}(t_0) = 0$$

and u_0 is the imposed displacement.

The stated problem is highly non-linear but due to the very simple excitation it nevertheless admits an analytical solution (refer to (Oliveto et al., 2010) for the solution). The existence of the analytical solution is convenient but by no means essential because the equation of motion could be solved numerically at the expense of additional computational costs and of some loss in precision.

The parameters that define the mechanical model are shown in Fig. 1, and for convenience are listed in the following vector: $(m, c, k_0, k_1, u_y, f_d)$. They represent the basic physical properties that must be identified. However, in view of the form given to the solution in (Oliveto et al., 2010), a new set of parameters is defined as follows: $(\omega_0, \omega_1, u_d, u_y, \zeta_0)$. This is related to the previous one by the following relationships:

$$\omega_0 = \sqrt{\frac{k_0}{m}}, \quad \omega_1 = \sqrt{\frac{k_1}{m}}, \quad u_d = \frac{f_d}{k_0}, \quad \zeta_0 = \frac{c}{2m\omega_0}$$

From Eq. (1) it can be inferred that three related response functions could be used for identification purposes: the displacement $u(t)$, the velocity $\dot{u}(t)$, and the acceleration $\ddot{u}(t)$. For the application at hand, the acceleration is the function that can be measured most easily and therefore is the one that will be used.

As already mentioned an initial displacement u_0 is imposed in the dynamical tests. Since the measurement of u_0 can be difficult it may be considered as an additional parameter that must be identified. Therefore, the system parameter vector to be optimised is the following one: $S = (u_0, \omega_0, \omega_1, u_d, u_y, \zeta_0)$

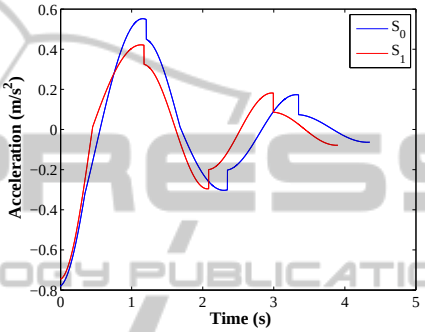

Figure 2: Acceleration functions corresponding to the sets of system parameters shown in Table 1.

Let A_0 be a vector of accelerations and t_0 be the vector of the corresponding times. Furthermore, let A be a vector of the same length as A_0 and t the vector of the corresponding times representing a candidate solution. Then, a measure of the distance between the experimental data and the modelled ones is provided by the following expression:

$$e^2 = \frac{(A_0 - A, A_0 - A)}{(A_0, A_0)} + \frac{(t_0 - t, t_0 - t)}{(t_0, t_0)}$$

where $(A,B) = \sum_{i=1}^{N} A_i \cdot B_i$ and N is the length of the considered vectors.

2.2 Previous results

Before applying the iterative least squares method to the experimental data, in (Oliveto et al., 2010) the procedure was tested on a mathematically generated dataset. In such a way, the optimal solution was known beforehand and the measurement noise excluded. Two system parameter vectors were defined so that one could be used to generate a set of experimental (analytical) data (i.e. S_1), and the other to define the starting point of the identification process

Table 1: First line: the two sets of system parameters considered in Fig. 2. S_1 is also the solution vector of the Test problem. Second line: range of admissible values for the system parameters. Third line: performance of the identification procedure according to the number of branches considered.

System	-	u_0(m)	ω_0(Hz)	ω_1(Hz)	u_d(m)	u_y(m)	ζ_0
S_0	-	0.12	0.50	0.40	0.005	0.02	0.05
S_1(opt)	-	0.12	0.55	0.35	0.004	0.03	0.03
Lower Bound	-	0.10	0.52	0.24	0.003	0.02	0.01
Upper Bound	-	0.14	0.58	0.48	0.005	0.04	0.05
Branches	Error						
1	$9.0981 \cdot 10^{-17}$	0.12	0.5500	0.3500	0.0040	0.0300	0.0300
1-2	$9.4827 \cdot 10^{-10}$	0.12	0.5500	0.3500	0.0040	0.0300	0.0300
1-2-3	$5.4252 \cdot 10^{-5}$	0.12	0.5503	0.3520	0.0038	0.0296	0.0338
1-2-3-4	$2.4896 \cdot 10^{-4}$	0.12	0.5509	0.3534	0.0037	0.0294	0.0372

(i.e. S_0). The two vectors are given in Table 1 and the related acceleration series are shown in Fig. 2.

The observation of Fig. 2 shows two kinds of discontinuities in the acceleration graphs, a function discontinuity and a slope discontinuity. Between two function discontinuities a continuous branch can be identified. The two graphs show the same number of branches; however, depending on the values of the system parameter vector the number of branches can be different.

Table 1 shows the results obtained in (Oliveto et al., 2010) with the iterative least squares method for the test problem. Better results are obtained by using only one or two branches of the acceleration record as may be seen from the error amplitude and by the coincidence of the identified parameters with the assumed ones. As the number of branches included in the identification procedure increases so does the error and the identified parameters are no longer coincident with the assumed ones.

The iterative least squares procedure described in (Oliveto et al., 2010) is based on the numerical calculation of the gradients of the test functions with respect to the system parameters (refer to (Oliveto et al., 2010), equations (29) – (35) for the actual procedure). A suitable arc length is chosen in the trial system parameter vector space by appropriately modifying the system of equations so that each component of the unknown vector is dimensionless. In order to make the procedure efficient it is necessary to "manually" reduce the "arc length" as the procedure converges and the error becomes smaller.

Although there certainly is no presence of noise and the function to be identified does "fit" the model, the best found solution exhibits an error of the order of 10^{-4}. The identified parameters differ from the given ones already at the third decimal digit. This is far from desired and excludes obtaining better results for the real data recorded at Solarino for the presence of noise and modelling errors.

A main problem in applying the least squares method or any optimization method is the definition of the starting point which in the case shown above was the set of parameters in Table 1 corresponding to the acceleration graph denoted by S_0 in Fig. 2. In practice this problem can be overcome by providing suitable lower and upper bounds to the sought parameters. This can be done by using physical insight on the observation of the given acceleration record. The bounds are shown in Table 1.

2.3 Evolution Strategies

The first applications of ESs were directed towards the parameter optimisation for civil engineering simulation models e.g. simulating stress and/or displacement states of structures under load (Schwefel, 1993). Obviously the performance of the ESs was compared against their natural competitors i.e. the mathematical methods used for the purpose, especially those not requiring the use of derivatives explicitly (Schwefel, 1993). Similarly, in the next section the performance of ESs will be compared against the methods applied in (Oliveto et al., 2010) on the same mathematically generated dataset (i.e. the test problem). To this end, first it will be seen how very simple ESs perform on the problem and then more complicated versions such as the CMA-ES will be applied.

A general $(\mu \dot{+} \lambda)$-ES maintains a *parent population* of μ individuals, each consisting of a *solution vector* and of a *strategy vector*. The solution vector represents the candidate solution to the optimisation problem. The strategy vector is a set of one or more parameters that are used in combination with the solution vector to create new candidate solutions.

In the considered problem an individual is represented as $(\mathbf{x}, \mathbf{s})$ where the solution vector $\mathbf{x} = (x_1, x_2, \ldots, x_6) \in \mathbb{R}^6$, is a real-valued vector for the candidate solution of the system parameter vector $\mathbf{S}$ introduced in Section 2. The initial μ solution vectors are generated uniformly at random within the parameter bounds given in Table 1.

Table 2: Average (Avg), Minimum (Min) and Median (Med) fitness found by 100 algorithm runs. (a) (1+1)-ES with no adaptation; (b) (1+1)-ES with no adaptation with normalised vectors; (c) (1+1)-ES with normalised vectors and rejecting points with fitness $f = 1$ as starting search point. The best results found are highlighted in **bold**.

	(a)	($\alpha = 1$)		**(b)**	($\alpha = 1$)	(Norm)	**(c)** ($\alpha = 1$)	(Norm)	($f_0 \neq 1$)
σ	Avg	Min	Med	Avg	Min	Med	Avg	Min	Med
10^{-5}	0.3455	5.03E-04	0.1257	0.4643	0.006	2.74E-01	0.28	5.60E-03	6.63E-02
10^{-4}	0.1108	**5.23E-05**	0.021	0.3218	7.80E-04	9.51E-02	0.1966	5.70E-03	5.73E-02
10^{-3}	**0.0255**	7.74E-05	**0.0028**	0.2553	**2.76E-05**	9.40E-03	0.012	1.44E-04	6.40E-03
10^{-2}	0.0475	4.85E-04	0.0093	0.0595	**4.51E-06**	**1.48E-04**	0.0025	8.89E-06	1.24E-04
0.025	0.2219	3.40E-03	0.00527	**0.0114**	**2.17E-05**	**1.25E-04**	**1.56E-04**	1.42E-05	1.33E-04
0.05	0.3778	6.10E-03	0.1403	**0.0097**	**4.24E-05**	**1.86E-04**	**2.52E-04**	4.04E-05	2.06E-04
0.1	0.342	1.00E-02	0.140	**4.79E-04**	**7.77E-05**	**4.45E-04**	**4.55E-04**	7.29E-05	4.19E-04
0.5	0.466	6.10E-03	0.278	0.0056	3.24E-04	5.10E-03	0.064	1.40E-03	6.00E-03

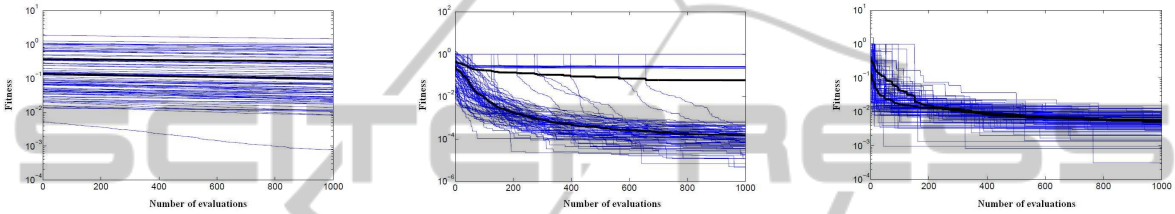

Figure 3: Fitness value versus number of evaluations of all the 100 runs (no adaptation and normalisation); (left) $\sigma = 0.0001$, (centre) $\sigma = 0.01$ and (right) $\sigma = 0.5$. The median and the mean are in bold.

In each optimisation step an *offspring population* of λ individuals is generated. Each individual is created by first selecting one of the μ individuals out of the parent population uniformly at random, and then by moving it in the search space of a quantity determined by applying its strategy vector **s**. The generation is completed by selecting the best μ individuals out of the parent and of the offspring populations if the *plus selection strategy* is used (i.e. (μ+λ)-EA) or out of the offspring population if the *comma selection strategy* is adopted (i.e. (μ,λ)-EA). The latter requires that λ be greater than μ.

The way the strategy vector **s** is applied to generate new individuals is explained when describing each ES considered in this paper. The main differences between various subclasses of ESs are in the size of the strategy vector, on how it is used and on how its values change during the optimisation process (i.e. *adaptation*).

3 TEST PROBLEM STUDY

In this section a study of popular ESs for the test problem considered in (Oliveto et al., 2010) is performed. Throughout the whole section (unless stated otherwise) each algorithm is run 100 times allowing 1000 fitness function evaluations in each run.

3.1 Experimental Setup: No Adaptation

The study begins by applying the simple (1+1)-ES and using a strategy vector consisting of only one strategy parameter σ (i.e. $\mathbf{s} \in \mathbb{R}^1$). The solution vector **x** of the parent individual ($\mathbf{x} \in \mathbb{R}^6$, σ) is initialised uniformly at random in the bounded search space. At each generation a new candidate solution is obtained by applying $\tilde{\mathbf{x}} := \mathbf{x} + \mathbf{z}$ where $\mathbf{z} := \sigma(\mathcal{N}_1(0,1), \ldots, \mathcal{N}_N(0,1))$ and $\mathcal{N}_i(0,1)$ are independent random samples from the standard normal distribution.

The only parameter of the algorithm is the standard deviation σ of the normal distribution used to generate the offspring solution vector. The value of σ does not change throughout the run of the algorithm. Given the "tight" bounds on the feasible search space provided in Section 2.2, the best *fixed* σ-values are expected to be small. By generating 100 random search points a minimum fitness (i.e. the error function value) of 0.0075 and an average fitness of 0.3950 are obtained. These values help to understand how well the algorithms are *fine-tuning* the initial solution.

The algorithm is tested for standard deviations σ distributed in the range $[10^{-6}, 5 \cdot 10^{-2}]$. The results are shown in Table 2 (a). The best solutions which are obtained for $\sigma = 0.001$ show average and minimum fitness of 0.0255 and of $7.74 \cdot 10^{-5}$ respectively.

Given the different value ranges for the bounds of each parameter, the solution is normalised according

Table 3: Effects of initial standard deviation σ^0 and 1/5 adaptation rule on Average (Avg), Minimum (Min) and Median (Med) fitness on 100 algorithm runs. (a) (1+1)-ES with 1/5 rule ($\alpha = 0.85$ and $G = 5$); (b) (1+1)-ES with 1/5 rule ($\alpha = 0.95$ and $G = 5$); (c) (1+1)-ES with "local" 1/5-rule. New Best results are highlighted in **bold**.

	(a) ($\alpha = 0.85$)			**(b)** ($\alpha = 0.95$)			**(c)** "local"-1/5		
σ^0	Avg	Min	Med	Avg	Min	Med	Avg	Min	Med
10^{-4}	0.0007	**1.750E-06**	1.52E-04	0.0029	**2.21E-06**	2.23E-04	3.15E-04	**2.41E-06**	2.20E-04
10^{-3}	**1.36E-04**	**9.45E-07**	**1.02E-04**	**1.54E-04**	**1.19E-06**	1.28E-04	3.47E-04	**2.60E-06**	1.87E-04
10^{-2}	0.0028	**2.10E-07**	**8.87E-05**	**1.20E-04**	**2.08E-07**	**7.97E-05**	0.0028	**2.64E-06**	1.72E-04
10^{-1}	0.0026	**1.90E-07**	**8.06E-05**	0.0047	**1.00E-06**	**7.01E-05**	0.0027	4.88E-06	2.04E-04
0.5	1.62E-04	**2.56E-06**	**1.18E-04**	**1.25E-04**	**7.24E-07**	**8.00E-05**	2.52E-04	**3.62E-06**	1.90E-04
1	1.57E-04	**1.47E-06**	**1.16E-04**	**1.35E-04**	**1.07E-06**	1.41E-04	0.0027	**2.01E-06**	1.74E-04

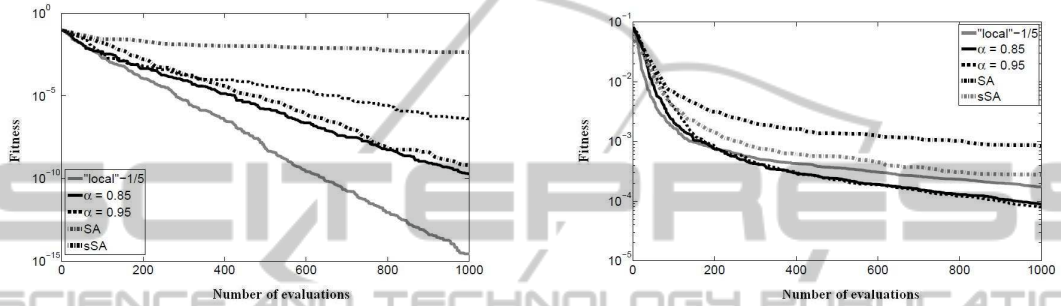

Figure 4: Performance of the three 1/5 success rule strategies, the isotropic (sSA) and the ellipsoidal (SA) on Sphere (left) and on the test problem (right) when $\sigma_0 = 0.01$. Median values out of 100 runs are plotted.

to $x_n = (x - \ell)/(u - \ell)$ where x_n is the normalised solution and u, ℓ are the upper and lower bound vectors on the solution space.

In Table 2 (b) the results for the (1+1)-ES using the normalised values are shown. If σ is too small the starting point does not get improved much whether the solution is normalised or not. However, for large enough σ values the normalised version outperforms the default one.

Examination of Table 2 (a) and (b) reveals a large difference between the average and the best solution. This indicates that the quality of the final solution may depend considerably on the random starting point. Fig. 3 shows the 100 runs for small, medium and large σ values. From the graphs it can be noticed how hard it is to escape from the penalty point (i.e. fitness=1) corresponding to a different number of branches between candidate and optimal solutions. A large σ is needed in order to escape. Table 2 (c) shows the results when such a point is rejected as a starting search point. If σ is not too small, the mean values are very close to the median ones, as desired.

In the following sections adaptation techniques are applied to remove the dependence of the results on the initial value of the standard deviation and achieve solutions of improved quality. For the rest of the paper, all the experiments are performed with the normalisation of the vector bounds and with rejection of starting points with different number of branches.

3.2 1/5 Rule Adaptation

One of the first methods proposed to control the mutation rate in an ES was the $1/5$-*rule* adaptation strategy (Beyer and Schwefel, 2002). The idea is to tune σ in a way that the *success rate* (i.e. the measured ratio between the number of steps when the offspring is retained and that when it is discarded) is about $1/5$. For the sphere function the $1/5$-rule has been proved to lead the (1+1)-ES to optimal mutation rates, hence optimal performance (Beyer and Schwefel, 2002).

The strategy works as follows. After a given number of steps G, the mutation strength (i.e. the standard deviation σ) is reduced by α if the rate of successful mutations $P_s := G_s/G$ is less than $1/5$. On the other hand, if $P_S > 5$, the mutation rate is increased by α. Otherwise it remains unchanged. Recommended values are $G = N$, if the dimensionality of the search space N is sufficiently large, and $0.85 \leq \alpha < 1$ (Beyer and Schwefel, 2002).

The $1/5$-rule strategy recently proposed by Kern et al. (Kern et al., 2003) that allows to update the step size after each generation rather than waiting until the end of the "window phase" G is also applied. In this simpler implementation, at each generation the step size is updated according to:

$$\sigma^{t+1} = \sigma^t \cdot \begin{cases} \alpha & \text{if } f(x^{t+1}) \leq f(x^t) \\ \alpha^{(-1/4)} & \text{otherwise.} \end{cases}$$

Here $\alpha = 1/3$ and the $(-1/4)$ in the exponent corresponds to the success rate of $1/5$.

The same (1+1)-ES of the previous section with the $1/5$-rule adaptation schemes are run with standard parameters. Table 3 shows the results for a wide range of initial standard deviations σ^0. The algorithm achieves mean fitness values and best solutions of the order of 10^{-4} and 10^{-7} respectively whatever the initial standard deviation σ^0 provided that it is not too small. Also the median results are considerably improved with values of the order of 10^{-5}.

Fig. 4 shows the performance of the different $1/5$-rule algorithms considered on the Sphere function and on the test function respectively. While on the Sphere, the "local" $1/5$ success rule is optimal, this does not seem to be the case for the test problem at hand. The larger "window" of $G = 5$ leads to a better adaptation of the step size.

The step size adaptation is shown in Fig. 5 for the test problem and the runs which provide median results. It appears that the decrease of the step size in the "local" 1/5 rule is too fast while it is too slow with the "ellipsoidal" self adaptation technique introduced and discussed in the next section.

3.3 Self-adaptation

Self-adaptation has been introduced as a mechanism for the ES to automatically adjust the mutation strength, by evolving not only the solution vector but also the strategy parameters. The strategy vector is also mutated such that standard deviations producing fitter solutions have higher probabilities of survival, hence are evolved implicitly.

By still considering only one strategy parameter, a mutation with self-adaptation of individual $(\mathbf{x}, \sigma)$ involves first generating a new σ-value and then applying it to the object vector $\mathbf{x}$. This is done by setting $\tilde{\sigma} := \sigma \exp(\tau \mathcal{N}(0,1))$, $\mathbf{z} := \tilde{\sigma}(\mathcal{N}_1(0,1), \ldots, \mathcal{N}_N(0,1))$ and $\tilde{\mathbf{x}} := \mathbf{x} + \mathbf{z}$. Here $\tau = 1/\sqrt{2N}$ is generally recommended as standard deviation for $\tilde{\sigma}$ (Beyer and Schwefel, 2002). By using only one strategy parameter σ, the mutation distribution is isotropic, i.e. surfaces of equal probability densities are hyper-spheres (or circles for $N = 2$).

If N strategy parameters are used, individual step sizes for each dimension are obtained leading to ellipsoidal surfaces of constant probability density as the standard deviations evolve. With a strategy vector $\mathbf{s} := (\sigma_1, \ldots \sigma_N)$ a new individual is generated by setting:

$$\tilde{\mathbf{s}} := \exp(\tau_0 \mathcal{N}_0(0,1)) \cdot \left(\sigma_1 \exp(\tau \mathcal{N}_1(0,1)), \ldots, \sigma_N \exp(\tau \mathcal{N}_N(0,1))\right)$$

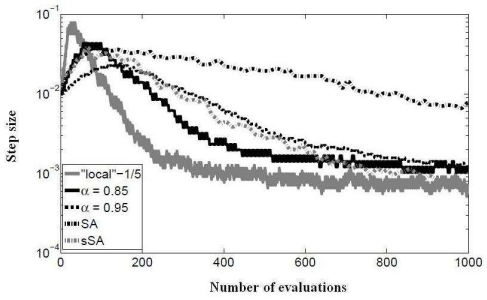

Figure 5: Step size evolution of the median fitness run for the three 1/5 success rule strategies, the isotropic (sSA) and the ellipsoidal (SA) on the test problem when $\sigma_0 = 0.01$.

and $\mathbf{z} := (\sigma_1 \mathcal{N}_1(0,1), \ldots, \sigma_N \mathcal{N}_N(0,1))$. Recommended values for the parameters are $\tau_0 = 1/\sqrt{2N}$ and $\tau = 1/\sqrt{2\sqrt{N}}$, (Beyer and Schwefel, 2002).

The results for both strategies, *isotropic* (sSA) and *ellipsoidal* (SA), are shown in Table 4, for the (1+10)-ES. The results are very similar for other offspring population sizes (from $\lambda = 3$ to $\lambda = 20$ were tested) both with plus and comma selection strategies. Concerning comma selection, bad average fitness values are achieved if the initial σ is too high (i.e. $\sigma > 0.5$) even though a penalty proportional to the distance from the bounds is applied for comma strategies.

Overall, comparable average performance to that of the (1+1)-ES with the "local" $1/5$-Rule is obtained independently of the initial values of σ as long as they are not too high or too low. Hence, not as much independence from the initial σ as with the $1/5$-rule is obtained. The typical evolution rate of σ is shown in Fig. 5 where it is compared with that of the $1/5$-rule. No significant improvement is achieved with the ellipsoidal distributions with axes parallel to the reference frame.

3.4 CMA-ES

Since the success of the described self-adaptation technique relies on one-step improvements it is often referred to as a *local adaptation* approach. By introducing *correlations* between the components of $\mathbf{z}$ the ellipsoid may be arbitrarily rotated in the search space and evolved to point in the direction of optimal solutions. Another step towards more advanced parameter adaptation techniques is to consider *non-local* information gathered from more than one generation. Both features are used by the (μ, λ)-CMA-ES considered in this section.

The CMA-ES creates a multivariate normal distribution $\mathcal{N}(\mathbf{m}, \mathbf{C})$ determined by its mean vector $\mathbf{m} \in \mathbb{R}^{\mathbb{N}}$ and its covariance matrix $\mathbf{C} \in \mathbb{R}^{\mathbb{N}\times\mathbb{N}}$. Instead of keeping a population of μ individuals (as in the pre-

Table 4: Results for the (1+10)-ESs.

	Isotropic	Mutations		Ellipsoidal	Mutations
σ^0	Avg	Min	σ_i^0	Avg	Min
10^{-4}	0.0032	1.54E-05	10^{-4}	0.0179	7.08E-05
10^{-3}	4.23E-04	7.59E-06	10^{-3}	0.0086	6.74E-05
10^{-2}	0.0031	2.91E-06	10^{-2}	0.0013	2.45E-05
0.05	3.17E-04	3.68E-06	0.05	9.38E-04	8.74E-06
0.1	3.02E-04	9.35E-06	0.1	69.25E-04	1.25E-05
1	0.0033	1.45E-05	1	0.0116	5.67E-05

Table 5: (a) Summary of best results found for the Test function with 1000 fitness function evaluations; (b) 10000 fitness function evaluations.

ES	adaptation	(a) Avg	Med	Min	(b) Avg	Med	Min
(1+1)-ES	No ($\sigma_0 = 0.01$)	0.0595	1.48E-04	4.51E-06	1.02E-05	8.35E-06	8.47E-07
(1+1)-ES	1/5rule ($\alpha = 0.95$, $G = 5$, $\sigma_0 = 0.01$)	1.20E-04	7.97E-05	2.08E-07	1.32E-08	2.36E-09	1.39E-12
(1+λ)-ES	self ((1+5)-ES, $\sigma_0 = 1$)	0.0023	3.54E-04	2.30E-06	7.89E-05	5.69E-06	2.16E-08
CMA-ES	non-loc. rot. ellips. self.	2.51E-05	5.79E-06	2.35E-10	2.22E-15	5.66E-16	2.14E-16

viously considered ESs), the covariance matrix $\mathbf{C}$ and the mean vector $\mathbf{m}$ are evolved. At each step λ individuals are sampled from $\mathcal{N}(\mathbf{m}, \sigma^2\mathbf{C})$ and the best μ are used to generate the new mean $\tilde{\mathbf{m}}$ and covariance matrix $\tilde{\mathbf{C}}$. For further details on the CMA-ES refer to (Hansen and Ostermeier, 2001).

In the present experiments, all the algorithmic parameters are set as recommended in (Hansen and Ostermeier, 2001) including $\lambda = 4 + \lfloor 3 \ln N \rfloor$ and $\mu = \lambda/2$. In the experiment set on the test problem as previously described the CMA-ES provided a set of solutions with mean $2.51 \cdot 10^{-5}$, median $5.79 \cdot 10^{-6}$ and minimum $2.35 \cdot 10^{-10}$ thus outperforming other considered algorithms of an order of magnitude in mean and median and of more than three orders of magnitude concerning the minimum solutions. No improvements are obtained by increasing or diminishing the population size (i.e. values from (1,4)-CMA-ES through (3,6)-CMA-ES up to (8,16)-CMA-ES).

Finally, 100 runs of the best performing EAs each of 10000 fitness function evaluations were done. The results are shown in Table 5(b). On this set of runs the mean and best results scored by the CMA-ES are 10^{-15} and 10^{-17} respectively.

4 SOLARINO DATA

In July 2004, six free vibration tests under imposed displacement were performed on a four story reinforced concrete building, seismically retrofitted by base isolation. The nominal displacements varied from a minimum of 4.06cm to a maximum of 13.29cm in the six dynamic tests. Unfortunately, these may not be true displacements since they may include residual displacement from tests performed previously in the sequence. The main objective, is the identification of the properties of the isolation system (i.e. the parameters of the previously described model) and the initial displacement as discussed above using the recorded accelerations.

The results obtained in (Oliveto et al., 2010) using an iterative least squares method are shown in Table 6. The procedure implied to start from a reasonable guess for the system parameters (for the identification of the first of the six tests), and use the first branch of the recorded acceleration for the identification of a new set of improved parameter values. This new set of parameters was then used for the identification from the first two branches and so on until five of the branches were considered at once. The last branch was derived from the governing equations using the parameters identified from the previous segments of the signal. For the identification of the following tests the result of the first test was used as the initial guess (i.e. the correct solution should be the same for all tests excluding damage of the building caused by the tests and/or effects due to environmental changes).

4.1 Previous Model

In this section advantage is taken of the simplicity of ES application and the ESs that performed best on the test problem are used. The parameter bounds to the search space are shown in table 6.

While the CMA-ES once again outperforms the other strategies, the difficulty of the identification problem is highlighted by the need to increase the population size to a (18,36)-CMA-ES to obtain improved results. Ten runs each are performed of (4,9), (9,18) and (18,36) CMA-ES and of the three 1/5 rule ESs allowing 100k fitness evaluations in each run.

Table 6: Identification of the Solarino building base isolation system. Used lower and upper bounds of system parameters are shown in lines starting with LB and UB repectively. The best identification results obtained in the literature by the least squares (LS) method from five tests are shown first. The corresponding results obtained by the CMA-ES are shown next. The number of times the best found solution was obtained in the runs is shown in brackets next to the test number. Quadratic errors and improvement achieved by CMA-ES are shown in the last two columns.

Test	u_0 (m)	u_d (m)	u_y (m)	ζ_0	ω_0 (Hz)	ω_1 (Hz)	e^2	improvement
LB	0.0813	0.0018	0.0092	0	0.4832	0.2819	-	-
UB	0.1333	0.0069	0.0366	0.1	0.5651	0.4417	-	-
LS								
3	0.1108	0.0034	0.0181	4.5E-08	0.5235	0.3947	0.0234	-
5	0.1169	0.0034	0.0167	0.0127	0.5117	0.4070	0.0105	-
6	0.1228	0.0035	0.0179	3.6E-08	0.5269	0.3909	0.0129	-
7	0.0927	0.0033	0.0173	3.87E-08	0.5222	0.3964	0.0122	-
8	0.0965	0.0025	0.0118	0.0306	0.5402	0.4242	0.0055	-
ES								
3 (4)	0.1063	0.0026	0.0132	1E-10	0.5507	0.4014	0.0147	37%
5 (2)	0.1153	0.0025	0.0127	0.0153	0.5384	0.4108	0.0049	53%
6 (2)	0.1122	0.0027	0.0130	1E-10	0.5559	0.4036	0.0096	25%
7 (3)	0.0856	0.0030	0.0132	1E-10	0.5455	0.4130	0.0106	13%
8 (4)	0.0976	0.0026	0.0109	0.0307493278	0.5382	0.4235	0.0052	5%

Starting from parent population sizes of $\mu = 9$ the CMA-ES converges more than once to the same solution.

Table 6 shows the best found solutions and the number of times they were repeated. The other solutions do not differ significantly from the best ones but for slightly larger errors and final parameter digits. Compared to the results from previous work, closer bounds for the likely real values of the parameters are now established.

The nominal values of the initial displacements, in all likelyhood affected by measurement errors, are given for each test in (Oliveto et al., 2010) together with the identified ones. The estimated displacements were always smaller than the nominal ones; here they are found even smaller, except for test 8.

In three tests out of five damping (ζ_0) is practically zero in line with what found in (Oliveto et al., 2010), while in the remaining two ζ_0 is small but not negligible and a little larger than in (Oliveto et al., 2010). This presence of damping in tests 5 and 8 could point to an incapacity of the optimization procedures to identify the absolute minimum, producing instead local minima. Alternatively, data inconsistency due to measurement noise and/or inadequate signal treatment could be responsible for the discrepancy.

The remaining physical parameters show less dispersion in the identified values than before, with a coefficient of variation nearly halved in each case. Actual values change from 0.13 to 0.07 for u_d, from 0.16 to 0.08 for u_y, from 0.02 to 0.01 for ω_0 and from 0.03 to 0.01 for ω_1. The situation could improve even further if the inconsistency highlighted by damping could be solved.

From the results shown in Table 6 and as commented above, a considerable improvement in the identification procedure has been achieved by using ES with the Solarino test data. In particular the results are improved up to 53% compared to those previously available in literature. The performance discrepancy of ES between the test problem and the real problem seems to suggest that further improvements might be required in the formulation of the mechanical model. Some preliminary investigations in that direction are pursued in the next section.

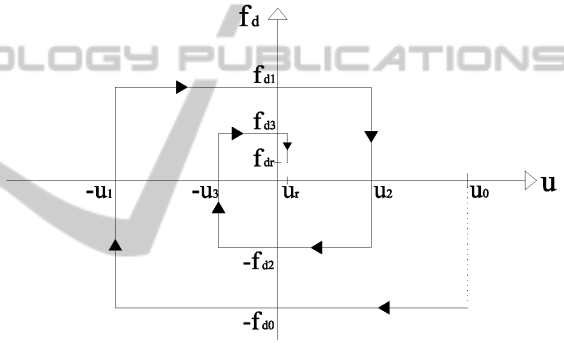

Figure 6: Model 2 friction force-displacement relationship.

4.2 New Models

Two small changes to the described model are investigated herein. They affect only the description of the friction damper of Fig.1 and will reflect in changes to the diagram of Fig. 1(c). The changes stem from the experimental observation that the friction force is not constant during the motion. The diagram of Fig.5 assumes that the friction force is constant within a half-

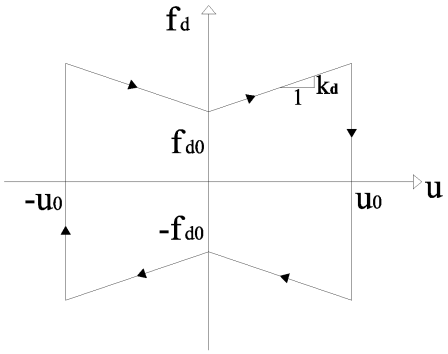

Figure 7: Model 3 friction force-displacement relationship.

cycle of motion but it can change from one half-cycle to the next. The considered change does not affect the equations of the mechanical model as it only changes one parameter value, but not the structure of the problem. However the dimension of the system parameter vector is affected because an additional parameter is required for each half-cycle of motion as compared to the single one required earlier.

The considered model, for convenience denoted model 2, provides results improved only slightly by running the CMA-ES on it (i.e. quadratic error reduced from 0.0147 to 0.0145 on test 3). Contrary to the previous model 1 the CMA-ES does not seem to succeed to repeat results in more than one run on model 2. This may be due to the greatly increased dimension of the problem (number of parameters nearly doubled) and to having maintained the same number of function evaluations (100k). The feeble success with this model may be due to two factors; the first is the computational expensiveness due to the higher dimension of the problem, the second is the insignificant mechanical advantage because the friction force changes more within a half-cycle than it does from half-cycle to half-cycle. The latter aspect will be clearer with the introduction of model 3.

An analytical solution for the mechanical model shown in Fig.1 with the friction law sketched in Fig.6 has just been given in (Athanasiou and Oliveto, 2011). This third model helps to spread some light on the little efficiency of model 2. While in model 3 the friction force varies linearly over a half-cycle, in model 2 the friction force is constant over the same half-cycle. It can be expected therefore that model 3 can fine tune the friction force much better than model 2 and for that matter much better than model 1, where the friction force is of constant amplitude. All this is achieved at the expense of only one additional parameter, the slope k_d in Fig.6. The application of the (18,36)-CMA-ES with Model 3 to Test 3 converges 4 times out of 10 to a solution with quadratic error $e^2 = 0.0139$ which is an extra improvement of more than 5% on the final fitness.

5 CONCLUSIONS

A study of ESs for the identification of base isolation systems in buildings designed for earthquake action has been presented. The results clearly show that ESs are highly effective for the optimisation of the test problem defined in previous work for methodology validation. All the considered ESs perform at least as well as previous methods and the quality of solutions improves with more sophisticated adaptation strategies. The CMA-ES, considerably outperforms previous algorithms of several orders of magnitude.

Having established the good performance of ESs for the system identification, the same ESs are applied to the real data recorded on the Solarino building in July 2004 with the model used previously in literature. Although the CMA-ES converges to more precise solutions, these do not allow the sought system parameter values to be established with the highest confidence level. Two possible causes have been considered: the presence of noise in the recorded data (i.e. the function to be optimised) and the model adequacy to properly simulate the system response.

To investigate the latter problem two new mechanical models with higher number of parameters have been developed. Both models, in conjunction with the application of CMA-ES, enable to obtain improved results. Model 3 allows fine tuning friction damping and provides a 5% improvement in the overall solution quality on Test 3.

Thus, in this paper ESs are shown to be a very powerful tool for the dynamic identification of structural systems. In particular, the CMA-ES combines application simplicity with convergence reliability. In view of the effectiveness shown in the applications considered in the present work, the authors believe that CMA-ES could be used advantageously with more complex models and various excitation sources including environmental ones. Presently improved models are under development as a replacement of the bi-linear description of rubber isolators.

REFERENCES

Athanasiou, A. and Oliveto, G. (2011). Modelling hybrid base isolation systems for free vibration simulations. In *Proc. of 8CUEE*, pages 1293–1302, Tokyo, Japan.

Beyer, H.-G. and Schwefel, H.-P. (2002). Evolution strate-

gies, a comprehensive introduction. *Natural Computing*, 1:3–52.

Hansen, N. and Ostermeier, A. (2001). Completely derandomized self-adaptation in evolution strategies. *Evolutionary Computation*, 9(2):159–195.

Kern, S., Müller, S. D., Hansen, N., Büche, D., Ocenasek, J., and Koumoutsakos, P. (2003). Learning probability distributions in continuous evolutionary algorithms - a comparative review. *Natural Computing*, 3:77–112.

Oliveto, N. D., Scalia, G., and Oliveto, G. (2010). Time domain identification of hybrid base isolation systems using free vibration tests. *Earthquake engineering and structural dynamics*, 39(9):1015–1038.

Schwefel, H. P., editor (1993). *Evolution and Optimum Seeking: The Sixth Generation*. Wiley & Sons, NY, USA.